CrossMark

ORIGINAL PAPER

The advantages of live/real time three-dimensional transesophageal echocardiography during assessments of pulmonary stenosis

Tuğba Kemaloğlu Öz[1] · Fatma Özpamuk Karadeniz[1] · Şükrü Akyüz[1] ·
Şennur Ünal Dayı[1] · Aycan Esen Zencirci[1] · Işıl Atasoy[1] · Altuğ Ösken[1] ·
Mehmet Eren[1]

Abstract This report sought to compare live/real-time three-dimensional transesophageal echocardiography (3D-TEE) with two-dimensional transesophageal echocardiography (2D-TEE) and to determine whether there are advantages to using 3D-TEE on patients with pulmonary stenosis (PS). Sixteen consecutive adult patients (50 % male and 50 % female; mean age 33 ± 13.4 years) with PS and indications of TEE were prospectively enrolled in this study. Following this, initial 2D-TEE and 3D-TEE examinations were performed, and 3D-TEE images were analyzed using an off-line Q-lab software system. Finally, the 2D-TEE and 3D-TEE findings were compared. In the present study, 3D-TEE allowed us to obtain the en face views of pulmonary valves (PVs) in all but one patient. While this patient was without a PV due to a previous tetralogy of Fallot operation, we could detect the type of PV in the other 15 (93.7 %) patients by using 3D-TEE. Due to poor image quality, the most stenotic area was not measurable in only one (6.2 %) of the patients. In eight (50 %) of the patients, severity and localization of stenosis were more precisely determined with 3DTEE than with 2D-TEE. The PVs' maximal annulus dimensions were found to be significantly larger when they were measured using 3D modalities. This study provides evidence of the incremental value of using 3D-TEE rather than 2D-TEE during assessments of PS, specifically in cases where special conditions (pregnancy, pulmonary regurgitation, and concomitant atrial septal defects) cause recordings of the transvalvular peak gradient to be inaccurate. Therefore, 3D-TEE should be used as a complementary imaging tool to 2D-TEE during routine echocardiographic examinations.

Introduction

The pulmonary valve (PV) is a semilunar valve with three cusps. It is located at the antero-superior and slightly to the left of the aortic valve (AV). Its cusps are much thinner than the AV and lack a fibrous continuity with the anterior leaflet of the right atrioventricular valve (tricuspid valve) [1–5].

Pulmonary stenosis (PS) is described as lesions that are collectively associated with obstructions to the right ventricular outflow tract (RVOT). These obstructions can be subvalvular, valvular, or supravalvular. PS is the most common problem related to the PV and occurs in approximately 10 % of all adult patients with congenital heart disease [6]. PV stenosis is generally congenital, and the stenotic valve can be unicuspid, bicuspid, or tricuspid [7]. Acquired lesions, which include tumors, endocarditis, rheumatic heart disease, and carcinoid heart disease, rarely involve the PV [8].

The initial evaluation of PS involves echocardiography. M-mode echocardiography, Doppler imaging, and two-dimensional echocardiography (2DE) are the most commonly used techniques for measuring the severity of PS [9]. Quantitative assessments of PS severity are primarily

✉ Tuğba Kemaloğlu Öz
tugbakemalogluoz@gmail.com

[1] Cardiology Department, Dr. Siyami Ersek Thoracic and Cardiovascular Surgery Training and Research Hospital, Kadıköy, Tıbbiye Cd No: 13, Istanbul, Turkey

based on the transpulmonary pressure gradient. Calculation of a PV's area by planimetry is not possible using 2DE because the required image plane is generally unavailable [10]. Additionally, the valvular gradient can be affected by multiple conditions, such as heart rate, regurgitation, and volume overload.

Typically, because only one or two leaflets of the PV can be visualized, and 2DE is generally unable to acquire en face views, determination of PV morphology is impossible. A three-dimensional reconstruction of a PV could help to visualize each of its leaflets and calculate its area. Therefore, the aim of the report was to compare real-time three-dimensional transesophageal echocardiography (3D-TEE) with two-dimensional transesophageal echocardiography (2D-TEE) and to determine whether there were advantages to using 3D-TEE on patients with PS. To the best of our knowledge, this is the first study to compare 2D-TEE and 3D-TEE findings from patients with PS.

Materials and methods

Study population

The first, eighteen patients who had been diagnosed with PS during routine 2D transthoracic echocardiography examinations in Dr. Siyami Ersek Thoracic and Cardiovascular Surgery Training and Research Hospital were enrolled prospectively between September 2013 and March 2015. In this single center study, inclusion critea were (1) age > 18 years, (2) who had indication for TEE and exclusion criteria was (1) not want to be included in the study. Of these, two patients who had not indication for TEE were excluded. All patients were in sinus rhythm, and the mean age of the patients was 33 ± 13.4 years old. Following this, initial 2D-TEE and 3D-TEE images were acquired for further evaluation. The 3D-TEE images were then analyzed, and the 2D-TEE and 3D-TEE data were compared.

Treatment for each patient was conducted according to the European Society of Cardiology's Guidelines for the management of grown-up congenital heart disease [11]. Before operation or valvuloplasty, right side cardiac catheterization was performed, and transvalvular peak-to-peak gradients were recorded. The protocol was approved by the institutional review board. Each participant gave their informed and written consent before enrollment in this study.

2D-TEE examinations

2D-TEE was performed on each patient with the Philips iE33 ultrasound system (Philips Medical Systems, Bothell, WA, USA) and the X7-2t matrix-array transducer. Examinations were conducted while patients rested in the left decubitus position. Mid-esophageal ($\sim 30°$–$45°$), upper-esophageal ($\sim 90°$), and transgastric ($\sim 0°$) views were used to obtain complete qualitative and quantitative data that met the standards of the American Society of Echocardiography [12]. PS severity was classified using the European Association of Echocardiography's and the American Society of Echocardiography's recommendations [10]. Pulmonary annulus measurements were generally made from the mid-esophagus, at approximately $30°$–$45°$ views, and between the hinge points of the PV.

3D-TEE examinations

3D-TEE was performed in all subjects with the same machine Philips iE33 ultrasound system), same transducer (X7-2t matrix-array), and same procedure that was performed at the end of the routine 2D-TEE. The 3D images taken from the transgastric and mid- and upper-esophageal views were nearly identical to the views that were taken during 2D-TEE. They were each taken using full volume, zoom mode, live 3D, and full volume with the color Doppler. The images were adjusted to make the PV the central object of interest. Data acquisition was based on recommendations put forth by the American Society of Echocardiography and the European Association of Echocardiography, which included recommendations for display and image acquisition using three-dimensional echocardiography [13]. For all modes, acquisition of a minimum of four consecutive beats was performed with optimizations for sector size and volume size to achieve optimal frame rate.

The acquired 3D images were analyzed using software analysis systems (Q-lab Advanced Quantification software, Version 8.1, Philips Ultrasound, USA). Settings of gain, contrast, and brightness were adjusted to obtain an optimal image quality required for analyses of the PVs. In order to produce different cut planes (frontal, longitudinal, transverse, and oblique) from various angles and directions, the PVs' en face views were obtained using the 3D crop function. The valve area was defined as the narrowest orifice at the time of the maximal valve opening and was measured through off-line analysis of the best acquired 3D images. 3D color Doppler views were used to confirm the accurate areas of the valves. Pathological structures, such as the PV and PV annulus, were quantified using multiplanar reconstruction (MPR) and non-MPR modes.

With the exception of peak gradient and peak velocity, there are no cut-off points for the classification of PV stenosis. Additionally, there is no data regarding 3D-TEE examinations of PS. Therefore, we classified PS according to valve areas, such as aortic stenosis (<1 cm^2 = severe stenosis, 1–1.5 cm^2 = moderate stenosis, and >1.5 cm^2 = mild stenosis) [11]. All PVs were categorized based on leaflet

numbers, such as unicuspid, bicuspid, or tricuspid, and the reasons behind each case of stenosis were examined in detail. Furthermore, RVOT and supravalvular areas were used to determine the narrowest parts. From these short-axis views, we identified the left, right, and anterior leaflets according to their relationships with surrounding cardiac structures. The two leaflets attached to the septum are named the left and right leaflets. These correspond to the right and left leaflets of the AV, which they face. The third leaflet is called the anterior leaflet [5, 6]. The area and maximal diameter of the PV annulus (located between the hinge points of the PV) were measured from the en face view of the PV.

Two expert observers, who were blinded to each other, measured the areas and maximal diameters of the PVs, pulmonary arteries (PAs), and PV annuli that were recorded by the 3D image datasets. To accomplish the intra-observer variability analysis, the first observer repeated measurements for 4 weeks after the initial measurements were recorded. To accomplish the inter-observer variability analysis, the second observer measured the same data sets over a separate specified period of time.

Statistical analysis

Data was statistically analyzed using the Number Crunching Statistical System (NCSS), 2007 and Power Analysis and Sample Size (PASS), and 2008 Statistical Software (Utah, USA). Numeric variables were expressed as the mean $\pm$ 1 the standard deviation. In the descriptive analysis of data, means, standard deviations, and percentages were used. An intraclass correlation coefficient (ICC) was used for the statistical calculation of the intra- and the inter-observer variability. A p value of <0.05 was considered to be statistically significant.

Results

The echocardiographic characteristics of these patients are shown in Table 1. Two (#6, #8) patients were pregnant, three (#2, #7, #8) patients had secundum atrial septal defects (ASDs), two (#3, #9) patients had significant pulmonary regurgitation (PR), one (#14) patient had undergone a Ross procedure, one (#9) patient had undergone a tetralogy of Fallot operation as a child, and one (#12) patient had undergone metallic tricuspid and mitral valve replacement.

2D-TEE findings

During the 2D-TEE examinations, 11 (68.7 %) patients had severe PS, and 5 (31.2 %) patients had moderate PS. The PVs' average maximal gradients were 75.4 $\pm$ 29.4 mmHg.

According to the 2D-TEE tests, only one patient (#4) had supravalvular stenosis while the others experienced valvular stenosis. As mentioned earlier, en face visualizations of PV leaflets were typically not possible during the 2D-TEE examinations. Therefore, the areas of the valves could not be obtained. Additionally, leaflet types could not be detected. The PVs' maximal annuli dimensions (2.2 $\pm$ 0.4 cm) were also measured.

3D-TEE findings

3D-TEE allowed for the visualization of leaflets from both the PA and the ventricular aspects. Assessments of PV leaflets and commissures were obtained in all patients but patient #9, who was without a PV due to a previous tetralogy of Fallot operation. In addition, one patient (#2) had bicuspid PV, two patients (#1, #4) had unicuspid PV, and one patient (#14) had a degenerated homograft PV.

Due to poor image quality, the most stenotic area was calculated by planimetry in all patients but patient #10. The areas of the PVs (1.2 $\pm$ 0.6 cm^2) were measured by an experienced operator. One (6.2 %) patient had no PS, three (18.7 %) patients had mild PS, four (25 %) patients had moderate PS, and seven (43.7 %) patients had severe PS. There were discrepancies between the 2D- and 3D-TEE classifications of severity in six of the patients (#s 2, 3, 4, 6, 8, 9). In this group, *three patients had ASDs, two patients were pregnant (one of the pregnant patients also had an ASD), and two patients had hemodynamically significant pulmonary regurgitation.* Two of the patients (#2, #7) with ASDs underwent surgery. Surgical and 3D-TEE findings about the PVs were also similar in each patient, which means that the 3D-TEE data from patients with ASDs were confirmed by surgeons. Discrepancies between 2D- and 3D-TEE findings disappeared in pregnant patients (#6, #8) because transvalvular gradients and the class of stenosis severity reduced after delivery. Especially, patient #6's stenosis was found severe according to maximal gradient but the valve area was calculated 1.44 (moderate PS) by 3D TEE. The patient was pregnant so the most appropriate time for valvuloplasty could be very important, however, after examining the previous echocardiographic reports, valvuloplasty was not deemed necessary and as such the class of stenosis severity reduced after delivery.

Additionally, two patients (#3, #9) experienced increases in PV flow due to the coexistence of PR and because the severity of stenosis may have been overestimated by the Doppler study. According to the 2D-TEE, patient #4 had severe supravalvular stenosis. During the 3D-TEE examination, however, the area of this patient's PV was measured to be 1.2 cm^2 (moderate stenosis), and their PA was found to be hypoplastic. The treatment strategy was made according to 3D TEE and catheterization results so

Table 1 2D-TEE, 3D-TEE, and catheterization findings with the incremental value of 3D imaging

	Sex/age	2D-TEE	3D-TEE	Catheter/peak-to-peak gradient	Treatment	Incremental value
1.	42/F	Doming PV and severe valvular PS (peak gradient 74 mm Hg)	Doming unicuspid PV and severe valvular PS (area = 0.29 cm^2) (Fig. 1; Video S1)	80 mmHg (valvular)	Valvuloplasty	En face visualization of the PV, exact quantification of the valve area, and detection of the leaflet type and morphology
2.	47/F	Bicuspid aortic valve, secundum ASD, and moderate valvular PS (peak gradient 43 mmHg)	Bicuspid aortic valve, secundum ASD, bicuspid PV, total fusion of left and anterior cusps, and mild valvular PS (area = 1.96 cm^2) (Figs. 2, 3; Video S2)	17 mmHg (valvular)	Operation: bicuspid AV and PV, secundum ASD, and mild PS (Fig. 4)	En face visualization of the PV, exact quantification of the valve area, detection of the leaflet types and morphology, and an exact classification of stenosis severity
3.	47/M	Moderate valvular PS (peak gradient 49 mmHg) and significant PR	Tricuspid PV, mild valvular PS (area = 1.71 cm^2), and significant PR (VCA = 0.35 cm^2)	40 mmHg (valvular)	Follow up	En face visualization of the PV, exact quantification of the valve area, detection of the leaflet types and morphology, and an exact classification of stenosis severity
4.	31/M	Supravalvular severe PS (peak gradient 65 mmHg)	Unicuspid and degenerated PV, moderate valvular PS (area = 1.22 cm^2), and hypoplastic PA	40 mmHg (valvular); 80 mmHg (supravalvular)	Operation: hypoplastic PA	En face visualization of the PV, exact quantification of the valve area, detection of the leaflet types, classification of stenosis severity and localization, and an accurate determination of the PA
5.	22/M	Doming PV and severe PS (peak gradient 110 mmHg)	Doming tricuspid PV and severe valvular PS (area = 0.73 cm^2)	100 mmHg (valvular)	Valvuloplasty	En face visualization of the PV, exact quantification of the valve area, and detection of the leaflet types and morphology
6.	19/F	Doming PV and severe PS (peak gradient 65 mmHg)	Doming tricuspid PV and moderate PS (area = 1.44 cm^2)	Could not be recorded due to pregnancy. She was in her second trimester	Follow up after delivery peak gradient of the PV reduced to 37 mmHg	En face visualization of the PV, exact quantification of the valve area, detection of the leaflet types, and an accurate classification of stenosis severity
7.	21/M	Secundum ASD, doming PV, and moderate PS (peak gradient 52 mmHg)	Secundum ASD, doming tricuspid PV, and no significant PS (area = 2.80 cm^2)	16 mmHg (valvular)	Operation: no significant PS, tricuspid PV, and large secundum ASD	En face visualization of the PV, exact quantification of the valve area, detection of the leaflet types, and an accurate classification of stenosis severity
8.	18/F	Secundum ASD, doming PV, and moderate PS (peak gradient 48 mmHg)	Secundum ASD, doming tricuspid PV, and mild PS (area = 1.93 cm^2)	Could not be recorded due to pregnancy. She was in her second trimester	Follow up after delivery peak gradient of PV reduced to 30 mmHg and after closure of ASD peak gradient reduced to 20 mmHg	En face visualization of the PV, exact quantification of the valve area, detection of the leaflet types, and an accurate classification of stenosis severity
9.	33/M[a]	Significant PR and severe PS (peak gradient 71 mmHg)	Significant PR, no PV, and moderate RVOT stenosis (area = 1.36 cm^2)	No indication	Follow up	En face visualization of the RVOT, exact quantification of the RVOT area, and an accurate classification of stenosis severity and localization

Table 1 continued

	Sex/age	2D-TEE	3D-TEE	Catheter/peak-to-peak gradient	Treatment	Incremental value
10.	36/F	Doming PV and severe PS (peak gradient 80 mm Hg)	Doming tricuspid PV, restricted motion of all cusps, and incalculable PV area due to poor echogenicity	60 mmHg	Valvuloplasty	En face visualization of the PV and detection of the leaflet types and morphology
11.	43/F	Doming PV and severe PS (peak gradient 106 mmHg)	Doming tricuspid PV, thickened and almost fixed anterior cusp, and severe PS (area = 0.79 cm^2)	69 mmHg	Valvuloplasty	En face visualization of the PV, exact quantification of the valve area, and detection of the leaflet types and morphology
12.	38/F	Doming PV, severe PS (peak gradient 79 mmHg), moderate AR, and metallic prosthetic TV and MV	Doming tricuspid PV, partial fusion of anterior and right cusps, restricted motion of all cusps, and severe PS (area = 0.44 cm^2) (Figs. 5, 6; Video S3)	Could not be recorded due to presence of the metallic TV	Operation was advised to the patient, but she did not accept the recommendation	En face visualization of the PV, exact quantification of the valve area, and detection of the leaflet types and morphology
13.	18/M	Doming PV and severe PS (peak gradient 67 mmHg)	Doming tricuspid PV, restricted motion of all cusps, and severe PS (area = 0.98 cm^2)	65 mmHg	Valvuloplasty	En face visualization of the PV, exact quantification of the valve area, and detection of the leaflet types and morphology
14.	23/F[b]	Moderate PS (peak gradient 58 mmHg) and conduit degeneration	Degenerated homograft PV and conduit and moderate PS (area = 1.1 cm^2)	No indication	Follow up	En face visualization of the PV, exact quantification of the valve area, and detection of the leaflet types and morphology
15.	26/M	Doming PV, severe PS (peak gradient 160 mmHg), and severe hypertrophic RVOT	Doming tricuspid PV, restricted right cusp motion, almost fixed anterior cusp, and severe valvular and subvalvular PS (PV area = 0.6 cm^2, RVOTA = 0.79 cm^2) (Figs. 7, 8)	113 mmHg	Valvuloplasty	En face visualization of the PV, exact quantification of the valve area, detection of the leaflet types, and an accurate classification of stenosis localization
16.	64/M	Doming PV and severe PS (peak gradient 80 mmHg)	Doming tricuspid PV, partial fusion of all cusps, and severe PS (area = 0.76 cm^2)	70 mmHg	Valvuloplasty	En face visualization of the PV, exact quantification of the valve area, and detection of the leaflet types and morphology

AR Aortic regurgitation, *ASD* atrial septal defect, *MV* mitral valve, *PA* pulmonary artery, *PS* pulmonary stenosis, *PV* pulmonary valve, *RVOTA* right ventricular outflow tract area, *TV* tricuspid valve

[a] Patient who had intracardiac repair of tetralogy of Fallot

[b] Patient who had undergone Ross procedure

valvulplasty was not performed. These 3D-TEE results were supported by surgical findings.

In three patients (#4, #9, #15), 2D-TEE and 3D-TEE findings on the localization of stenosis produced different results. While patient #4's stenosis was found to be severe during 2D-TEE, their valvular PS and hypoplastic PA were found to be moderate according to the planimetric assessment with 3D-TEE. This finding was confirmed by the *surgeon*. In one patient (#9), while no signs of PV and only moderate RVOT stenosis were found during examination, the exact localization of stenosis was unclear during 2D-TEE. Additionally, although patient #15 experienced simultaneous and severe valvular and subvalvular stenosis, and the subvalvular area could be measured by 3D-TEE (Fig. 7), the exact localization of stenosis could not be detected with 2D-TEE.

Measurements of PV annuli were obtainable in all patients but patient #9, who did not have a PV. The average maximal dimensions of the PVs' annuli were 2.6 ± 0.5 cm. Additionally, and without exception, all maximal dimensions of the PVs' annuli were found to be statistically significant ($p = 0.001$) and larger when measured using the 3D modality. The mean area of the PVs' annuli was 4.3 ± 1.3 cm^2.

Table 2 Intra- and inter-observer variability

	ICC (intra)[a]	95 % CI	ICC (inter)[b]	95 % CI
PV annulus max diameter	0.843**	0.59–0.94	0.821**	0.55–0.94
PV annulus area	0.991**	0.97–0.99	0.991**	0.97–1.00
PV area	0.773**	0.45–0.92	0.967**	0.90–0.99
PA max diameter	0.979**	0.94–0.99	0.979**	0.79–0.99
PA area	0.994**	0.98–1.00	0.994**	0.98–1.00

ICC Intraclass correlation coefficient, *CI* confidence interval, *PA* pulmonary artery, *PV* pulmonary valve

** $p < 0.01$

[a] Intraobserver agreement

[b] Interobserver agreement

The average peak-to-peak gradient in the 11 (69.7 %) patients who underwent right heart catheterizations was 60.9 ± 30.9 mmHg. Percutaneous transluminal balloon *valvuloplasty* was attempted in seven (43.7 %) patients. Surgical intervention was scheduled in three (18.7 %) patients (#2, #4, #7) who had other indications for operations when the exact quantification of the valve area, localization of stenosis, and classification of stenosis severity had been confirmed at the time of surgery for each patient (100 %). Operation was advised to patient #12 because she had moderate aortic regurgitation and had previously undergone tricuspid and mitral valve replacement. Close monitoring of five (31.2 %) of the patients was suggested.

Intra- and inter-observer variability

Excellent inter- and intra-observer correlation were found for 3D-TEE measurements of the areas and maximal diameters of PVs, PAs, and PV annuli (see Table 2).

Discussion

To the best of our knowledge, this is the first report to apply 3D-TEE for the assessments of RVOT, supravalvular area, PS, PV, and PV annulus features, and the first study to compare its findings with those obtained from 2D-TEE examinations. Likewise, our recent report focuses on the morphologies of PVs and PS. In providing incremental values in the identification and characterization of PVs, this study presents further evidence of the advantages of 3D-TEE over 2D-TEE.

3D-TEE data that were obtained from the en face views of PVs provided the ability to differentiate between unicuspid, bicuspid, and tricuspid leaflet morphologies. Thus far, few data assessments of PV have been conducted with three-dimensional transthoracic echohocardiography (3D-TTE). For example, Anwar et al. [14] performed 3D-TTE examinations on 50 patients with complex congenital heart disease and detected bicuspid PVs in three of the patients. The researchers also obtained excellent visualizations of the PVs in 12 (24 %) of the patients. Kelly et al. studied 200 consecutive patients who were referred for routine TTE examinations. 3D-TTE examinations showed the morphological characteristics of three cusps through en face views of 60 % of the study's patients [15]. In another study, which included five patients with PS who had been tested with 2D-TTE and 3D-TTE, three of the patients' PV areas were obtained by planimetry (60 %) [16].

In our study, the en face views of PVs were visible in 15 of the patients (93.7 %; patient #9 had no PV). Due to poor image quality, the most stenotic area was unobtainable in only one patient (#10; 6.2 %). Based on our data, both the percentage of successful visualizations of PVs and the calculation of their most stenotic areas were higher than in previous reports. However, we used 3D-TEE data rather than 3D-TTE data to record our findings. To date, only four *case reports* have published the use of *3D-TEE in examinations of PV* [17–20]. *One case report evaluated bioprosthetics in PVs* [17], another *case report evaluated bicuspid leaflets in PVs using 3D-TEE* [20], and *two case reports showed how 3D-TEE could be used to evaluate the structure and function of PVs during instances of carcinoid heart disease* [18, 19]. *Similar to our results, these case reports* provided evidence of the incremental value of 3D-TEE over 2D-TEE during assessments of PVs.

One of our study's main findings is that the classification of PS, according to the planimetric method, is better than classifications of the peak gradient and peak velocity. Unlike gradient and velocity [10], the planimetric method is not affected by flow rate. In this data, the planimetric method proved especially useful in patients with PR and ASDs. When a patient is affected by an ASD, and there are increases in *right atrial volume, right ventricular (RV) volume, and pulmonary blood flow* due to left to right shunts [10], their transvalvular gradients may be significantly elevated due to increased stroke volume across the valve. This same situation occurs during PR. Severe regurgitant volume also leads to relative stenosis and an
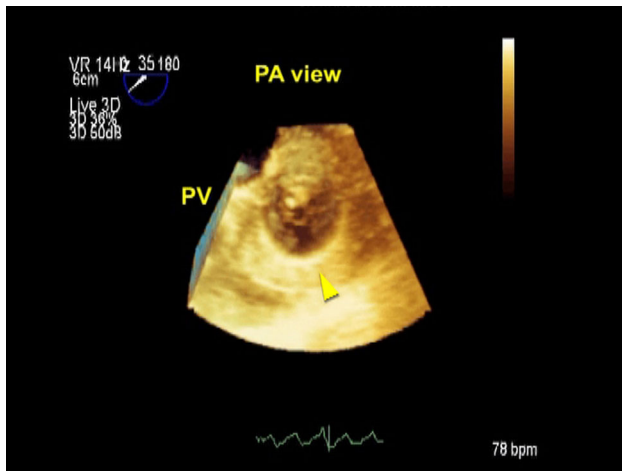
Fig. 1 *Case 1* A real-time three-dimensional transesophageal echocardiography, an en face view of the PV imaged from the PA, and an *arrow* head showing the PV (Fig. 1; Video S1). *PA* pulmonary artery, *PV* pulmonary valve
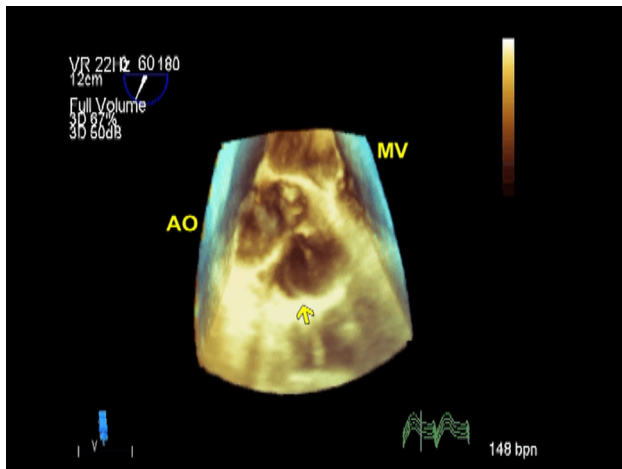

Fig. 2 *Case 2* A real-time three-dimensional transesophageal echocardiography and an en face view of the bicuspid PV (*arrow*) imaged from the PA (Fig. 2; Video S2). *AO* aorta, *MV* mitral valve

Fig. 3 *Case 2* A multiplane reconstruction mode and a calculation of the valve area (*arrow*). *AO* aorta, *AV* aortic valve, *TV* tricuspid valve

Fig. 4 *Case 2* An *arrow* pointing to the surgical view of the bicuspid PV

increase in transvalvular gradient. The other important patient population to consider is pregnant women. The indications for percutaneous balloon pulmonary valvuloplasty are usually based on the symptoms and the peak gradient (or peak velocity) of a PV [10]. Cardiac output and the amount of blood that passes through a PV increases during pregnancy [21]. The peak gradient and peak velocity of a PV can also be affected by pregnancies, which can lead to an overestimation of the severity of PS. Additionally, symptoms of severe PS, such as dyspnea and atypical angina, are common but not specific to pregnant patients. This misclassification may influence the accuracy of the time that it takes to perform valvuloplasties on o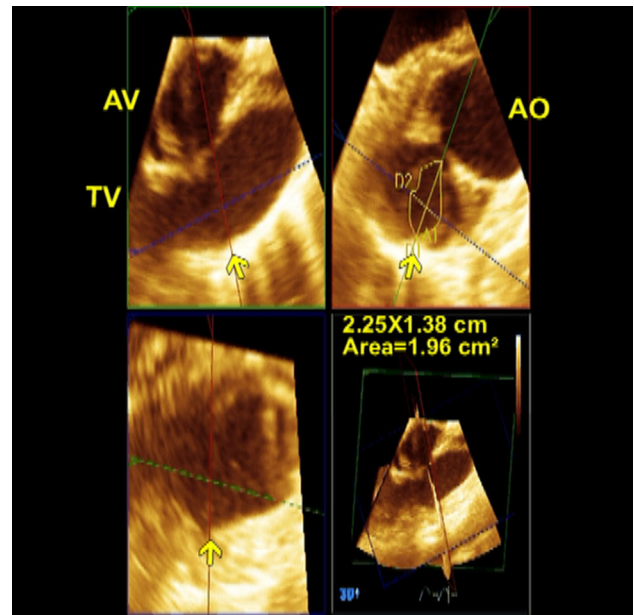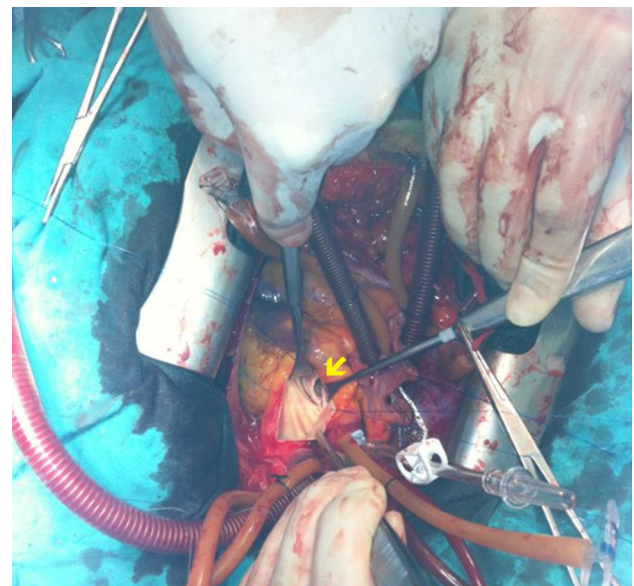ur pregnant patients (#6, #8). It may also lead to radiation exposure to fetuses, which can produce undesirable effects as a consequence. As in one patient (#6), because of the overestimation of severity of stenosis, the unnecessary valvuloplasty could be performed during pregnancy. Therefore, 3D-TEE examinations could prove safe and useful during situations where a patient is pregnant.

Conversely, transvalvular gradient levels may be low in the presence of significant stenosis. The combination of a
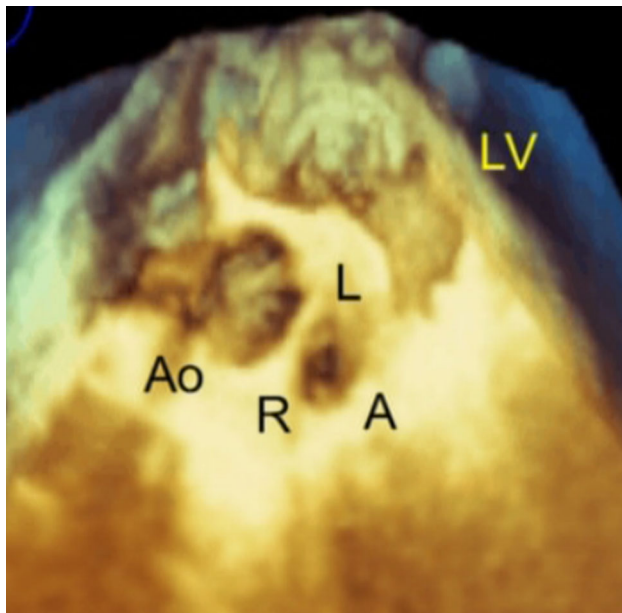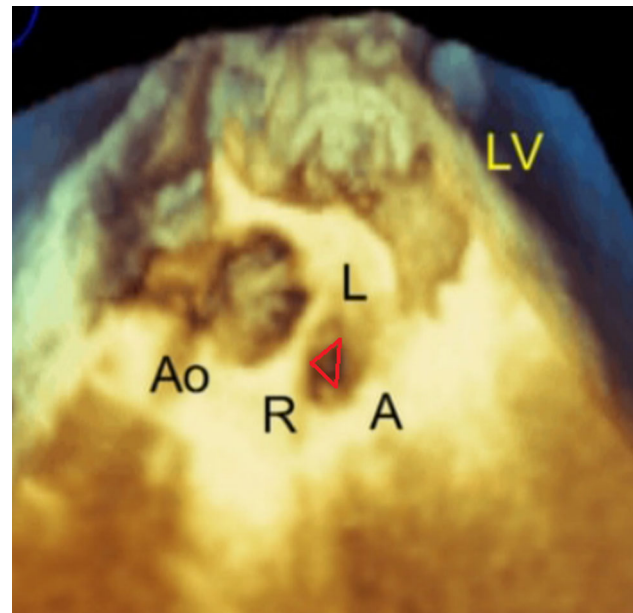
Fig. 5 *Case 12* A real-time three-dimensional transesophageal echocardiography and an en face view of the tricuspid PV imaged from the PA in systole (Fig. 5; Video S3). *A* anterior cuspis, *AO* aorta, *L* left cuspis, *LV* left ventricle, *R* right cuspis

Fig. 6 *Case 12* A real-time three-dimensional transesophageal echocardiography and an en face view of the tricuspid PV imaged from the PA in systole. The *red triangle* shows the PV's opening area. *A* anterior cuspis, *AO* aorta, *L* left cuspis, *LV* left ventricle, *R* right cuspis

3D-TEE test and 2D-TEE can also help to differentiate severe stenosis from other conditions in patients with poor RV systolic function (e.g. low flow/low gradient pulmonary stenosis).

The localization of a right ventricular outflow obstruction (RVOTO) is detected by using 2D-echocardiographic and Doppler techniques [9]. While a pulsed wave Doppler technique is generally apt at discriminating between subvalvular, valvular, and supravalvular stenosis [22], differential diagnoses can be difficult when there are two or more stenotic parts. Additionally, because the 2D bi-plane echocardiography takes thin, slice-like images of the PA and right ventricle structures, the 2D-TEE test's value in visualizing all anatomic aspects of the PV is limited. Using 3D-TEE, the entire PV and its subvalvular and supravalvular structures can be acquired, and the exact localization of RVOTO can be seen.

Other modalities, such as computerized tomography and magnetic resonance imaging (MRI), play an important role in the evaluation of PV disorders [23]. Although MRI scans are too expensive to be made readily accessible, they are especially useful during functional evaluations and quantifications of the hemodynamic consequences of PV abnormalities. Though painless, MRI scans can be unpleasant for patients who are claustrophobic or otherwise uncomfortable with the imaging device that surrounds them. After performing Ross procedures on 10 normal subjects, Kivelitz et al. [24] used a bright blood cine MRI to visualize the PVs in 14 patients. While the three leaflets could be visualized in all of the patients following the Ross operations, the entirety of the PVs' three leaflets could only be identified in the six normal subjects.

Using cardiac-gated computerized tomography angiographies, evaluation of both native and prosthetic PVs is now possible [25]. However, radiation exposure during these procedures remains a significant problem for pregnant patients. Therefore, 3D-TEE tests should be considered for assessments of PS. These examinations can be used on all patient groups (including pregnant women, claustrophobic patients, etc.) and are safe and relatively inexpensive imaging modalities.

In our study, all dimensions of PV annuli were larger when they were measured by the 3D-TEE modality. While 3D-TTE examinations have been used to record measurements of the PV annulus in only one published report, these measurements were obtainable from each of the patients same as our study [16].

Study limitations

Because operation was not the selected therapeutic strategy for a considerable number of patients, this study was limited by its inability to confirm certain data with gold standard methods such as surgery for validation and 3D-TEE findings. In addition, the sample size was limited, especially for the group with PS, because the study
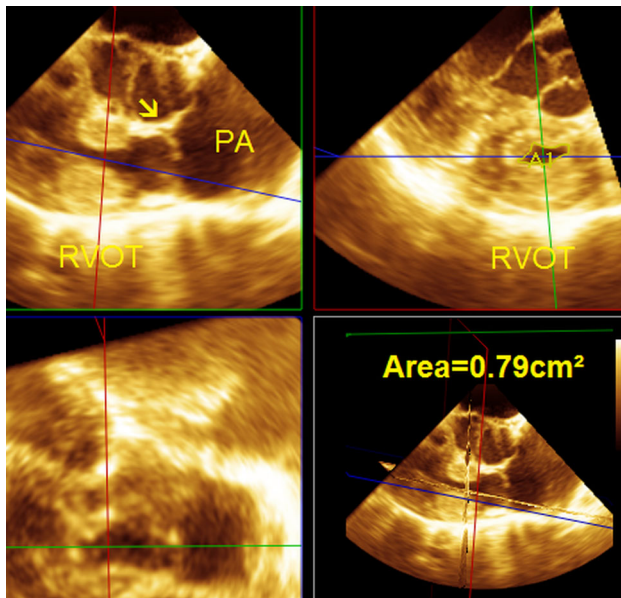
Conclusions

This study provides evidence of the incremental value of using 3D-TEE over 2D-TEE during assessments of PS, especially in encounters with specialized conditions (PR, pregnancy, and/or concomitant ASD) that can cause recordings of the transvalvular peak gradient to be inaccurate. This misclassification may influence the accuracy of the time and the necessary treatment strategies. 3D-TEE examinations are feasible, reproducible, and accurate techniques for measuring the PV areas in patients with PS. Therefore, 3D-TEE should be used as an imaging tool that compliments 2D-TEE during routine echocardiographic examinations.

Compliance with ethical standards

Conflict of interest The authors declare that they have no conflict of interest.

Fig. 7 *Case 15* A real-time three-dimensional transesophageal echocardiography, a multiplane reconstruction mode, and a calculation of the subvalvular area. The *arrow* shows the PV. *PA* pulmonary artery; *RVOT* right ventricular outflow tract
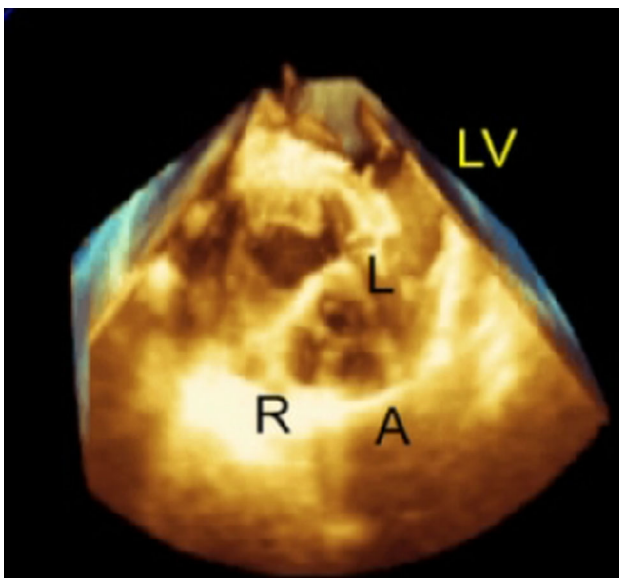

Fig. 8 *Case 15* A real-time three-dimensional transesophageal echocardiography that demonstrates an en face view of a tricuspid PV that was imaged from the PA in diastole. *A* anterior leaflet, *L* left leaflet, *LV* left ventricle, *R* right leaflet

consisted of either adults or patients with PS who had been treated before they were 18 years old. Despite these limitations, the study's results are of interest from a developmental perspective and add a new and potentially greater degree of accuracy for the quantitative measurement of the PV.

References

1. Goss CM, Gray H (1973) Valves of the heart. Gray's anatomy of the human body, 29th edn. Lea & Febiger, Philadelphia, pp 543–544
2. Gross L, Kugel MA (1931) Topographic anatomy and histology of the valves in the human heart. Am J Pathol 7:445
3. Barry A, Patten BM (1968) The structure of the adult heart. In: Gould SE (ed) Pathology of the heart and blood vessels, 5th edn. Charles C. Thomas, Springfield, p 91
4. Misfeld M, Sievers HH (2007) Heart valve macro- and microstructure. Philos Trans R Soc Lond B Biol Sci 362:1421–1436
5. Dominik J, Zacek P (2010) Heart valve surgery; an illustrated guide, 1st edn. Springer, Berlin, pp 40–41
6. Camm AJ, Lüsher TF, Serruys WP (2009) The ESC textbook of cardiovascular medicine, 2nd edn. Oxford University Press, New York, p 347
7. Waller BF, Howard J, Fess S (1995) Pathology of pulmonic valve stenosis and pure regurgitation. Clin Cardiol 18:45–50
8. Popelová J, Oechslin E, Kaemmerer H, Sutton MGJ, Žácek P (2008) Congenital heart disease in adults, 1st edn. Informa Healthcare, London, pp 87–89
9. Armstrong WF, Ryan T (2010) Feigenbaum's echocardiography, 7th edn. Lippincott Williams and Wilkins, Philadelphia, pp 337–359
10. Baumgartner H, Hung J, Bermejo J, Chambers JB, Evangelista A, Griffin BP et al (2009) Echocardiographic assessment of valve stenosis: EAE/ASE recommendations for clinical practice. Eur J Echocardiogr 10:1–25
11. Baumgartner H, Bonhoeffer P, De Groot NMS, Haan F, Deanfield JE, Galie N et al (2010) ESC guidelines for the management of grown-up congenital heart disease. Eur Heart J 31:2915–2957
12. Hahn RT, Abraham T, Adams MS, Bruce CJ, Glas KE, Lang RM et al (2013) Guidelines for performing a comprehensive transesophageal echocardiographic examination: recommendations from the American Society of Echocardiography and the Society of Cardiovascular Anesthesiologists. J Am Soc Echocardiogr 26:921–964

13. Lang RM, Badano LP, Tsang W, Adams DH, Agricola E, Buck T et al (2012) American Society of Echocardiography; European Association of Echocardiography. EAE/ASE recommendations for image acquisition and display using three-dimensional echocardiography. J Am Soc Echocardiogr 25(1):3–46

14. Anwar AM, Soliman O, Van Den Bosch AE, McGhie JS, Geleijnse ML, Cate FL (2007) Assessment of pulmonary valve and right ventricular outflow tract with real-time three-dimensional echocardiography. Int J Cardiavasc Imaging 23:167–175

15. Kelly NF, Platts DG, Burstow DJ (2010) Feasibility of pulmonary valve imaging using three-dimensional transthoracic echocardiography. J Am Soc Echocardiogr 23:1076–1080

16. Anwar AM, Nosir YF, Zainal-Abidin SK, Ajam A, Chamsi-Pasha H (2012) Real-time three dimensional transthoracic echocardiography in daily practice: initial experience. Cardiovasc Ultrasound 10:14

17. Ahmed MI, Escañuela MG, Crosland WA, McMahon WS, Alli OO, Nanda NC (2014) Utility of live/real time three-dimensional transesophageal echocardiography in the assessment and percutaneous intervention of bioprosthetic pulmonary valve stenosis. Echocardiography 31:531–533

18. Waller AH, Chatzizisis YS, Moslehi JJ, Chen FY, Mangion JR (2014) Real-time three-dimensional transoesophageal echocardiography enables preoperative pulmonary valvulopathy assessment. Eur Heart J Cardiovasc Imaging 15:713

19. Bhattacharyya S, Burke M, Caplin ME, Davar J (2011) Utility of 3D transesophageal echocardiography for the assessment of tricuspid and pulmonary valves in carcinoid heart disease. Eur J Echocardiogr 12:E4

20. Cho SW, Kim BG, Kim DH, Kim BO, Goh CW, Rhee KJ et al (2014) Three-dimensional echocardiographic views of bicuspid pulmonic valve. J Cardiovasc Ultrasound 22:162–163

21. Libby P, Bonow RO, Mann DL, Zipes DP (2008) Braunwald's heart disease, 8th edn. Sounders Elsevier, Philadelphia, pp 1577–1580 and 1967–1968

22. Cuypers JA, Witsenburg M, van der Linde D, Roos-Hesselink JW (2013) Pulmonary stenosis: update on diagnosis and therapeutic options. Heart 99:339–347

23. Rajiah P, Nazarian J, Vogelius E, Gilkeson RC (2014) CT and MRI of pulmonary valvular abnormalities. Clin Radiol 69:630–638

24. Kivelitz DE, Dohmen PM, Lembcke A, Kroencke TJ, Klingebiel R, Hamm B et al (2003) Visualization of the pulmonary valve using cine MR imaging. Acta Radiol 44:172–176

25. Saremi F, Gera A, Ho SY, Hijazi ZM, Sánchez-Quintana D (2014) CT and MR imaging of the pulmonary valve. Radiographics 34:51–71